Journal of Molecular Graphics and Modelling 28 (2009) 226–235

Contents lists available at ScienceDirect

Journal of Molecular Graphics and Modelling

journal homepage: www.elsevier.com/locate/JMGM

Modeling of high-affinity binding of the novel atrial anti-arrhythmic agent, vernakalant, to Kv1.5 channels

Jodene Eldstrom, David Fedida *

Department of Anesthesiology, Pharmacology and Therapeutics, University of British Columbia, 2350 Health Sciences Mall, Vancouver, British Columbia, Canada V6T 1Z3

ARTICLE INFO

Article history:
Received 17 February 2009
Received in revised form 25 July 2009
Accepted 27 July 2009
Available online 5 August 2009

Keywords:
Vernakalant
Atrial fibrillation
Kv1.5
AutoDock

ABSTRACT

Vernakalant (RSD1235) is an investigational drug that converts atrial fibrillation rapidly and safely in patients intravenously [Roy et al., J. Am. Coll. Cardiol. 44 (2004) 2355–2361; Roy et al., Circulation 117 (2008) 1518–1525] and maintains sinus rhythm when given orally [Savelieva et al., Europace 10 (2008) 647–665]. Here, modeling using AutoDock4 allowed exploration of potential binding modes of vernakalant to the open-state of the Kv1.5 channel structure. Point mutations were made in the channel model based on earlier patch-clamp studies [Eldstrom et al., Mol. Pharmacol. 72 (2007) 1522–1534] and the docking simulations re-run to evaluate the ability of the docking software to predict changes in drug–channel interactions. Each AutoDock run predicted a binding conformation with an associated value for free energy of binding (FEB) in kcal/mol and an estimated inhibitory concentration (K_i). The most favored conformation had a FEB of −7.12 kcal/mol and a predicted K_i of 6.08 μM (the IC50 for vernakalant is 13.8 μM; [Eldstrom et al., Mol. Pharmacol. 72 (2007) 1522–1534]). This conformation makes contact with all four T480 residues and appears to be clearly positioned to block the channel pore.

1. Introduction

Most drugs currently used for the treatment of atrial fibrillation are indiscriminate, targeting channels in both atrial and ventricular tissue and are associated with life-threatening (ventricular) arrhythmias as a consequence. Vernakalant (RSD1235) is the first of a new generation of mixed voltage- and frequency-dependent Na^+ and atria-preferred K^+ channel blockers [1,5,6] under development for the acute conversion of atrial fibrillation to sinus rhythm. Recent results from Phase IIb trials show promise for the oral use of vernakalant to suppress arrhythmia recurrence [3]. One important atrial K^+ current often thought of as a target for the treatment of atrial fibrillation, is I_{Kur}, the molecular correlate of which is the Kv1.5 channel [7,8]. In the first part of this study we investigated the binding site of vernakalant in Kv1.5 using primarily an experimental mutational approach [4]. Based on the results of an alanine mutation scan we identified several key residues in the S6 (I502, V505 and I508) and pore helix (T479 and T480) that, when mutated, resulted in modest to large changes in IC_{50} for vernakalant and flecainide. These residues showed a great deal of overlap with key residues shown to be involved in block by other compounds [9–13]. Electrostatic charge, size, hydrophobicity and ability to make cation–π interactions further appeared to influence the interaction between drug and channel, and the relative importance of these factors varied with the site within the channel [4].

Here, we used the crystal structure of Kv1.2 (which is 100% homologous in the inner vestibule to Kv1.5, Fig. 1) to allow us to interpret structurally the mutational data from our previous study. There are differences in the extracellular turret region between the two channels, but these residues are >20 Å from the binding site so are unlikely to play a role in vernakalant binding to Kv1.5. We have examined more completely binding of vernakalant as predicted by AutoDock4 and from these results we find it is probable that V505 and I508 in S6 and T479 and T480 in the pore helix can interact directly with vernakalant. Indeed, molecular modeling of the docking of vernakalant predicts that these residues, and some that were not predicted, are involved in the binding of the drug. One of the lowest energy conformations for drug–channel binding predicted by the Autodock program (designed to predict how small molecules, i.e. drugs, bind to a receptor of known 3D structure; http://autodock.scripps.edu/) suggests that M478, T480, V505 and I508 may bind vernakalant. Of interest, is that the program has predicted that in this conformation, vernakalant makes contact with every subunit in the tetrameric protein.

We have made some of the same mutations in the channel model that were tested in our earlier experimental study, energy minimized the residues around the change to allow recalculation

* Corresponding author at: Department of Anesthesiology, Pharmacology and Therapeutics, University of British Columbia, 2176 Health Sciences Mall, Vancouver, British Columbia, Canada V6T 1Z3. Tel.: +1 604 822 5806; fax: +1 604 822 2281.
E-mail address: fedida@interchange.ubc.ca (D. Fedida).

1093-3263/$ – see front matter © 2009 Elsevier Inc. All rights reserved.
doi:10.1016/j.jmgm.2009.07.005

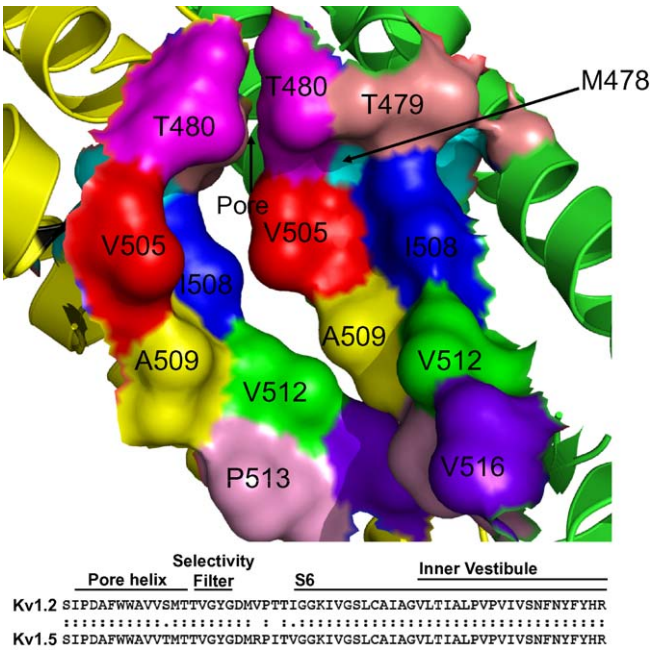

Fig. 1. Surface of inner vestibule of the Kv1.5 channel highlighting potential amino acids available for interaction. Potential interacting amino acids are in surface view while the rest of the two visible subunits are in cartoon format. Color code is M478 in cyan, T479 in salmon, T480 in purple, V505 in red, I508 in blue, A509 in yellow, V512 in green, P513 in pink and V516 in sky blue. Image adapted from the crystal structure of Kv1.2 (Long et al., 2005; [16]) using MacPyMOL (DeLano, W.L. MacPyMOL: A PyMOL-based Molecular Graphics Application for MacOS X, 2007, DeLano Scientific LLC, Palo Alto, CA, USA. http://www.pymol.org). Inner vestibule and p-loop alignment of Kv1.2 and Kv1.5. The alignment was created using l-align (http://www.ch.embnet.org/software/LALIGN_form.html).

of the protein structure, and performed the molecular docking again. This was to see if insight could be gained into how the mutations affected block by the drug, the model allowed us to observe how the architecture is changed and how this then affected the predicted binding sites.

2. Materials and methods

2.1. Docking

Blind docking was carried out using AutoDock4 software [14,15] using the default parameters, the Lamarkian genetic algorithm with local search and 25 million energy evaluations (Long evals) per run, using a MacBookPro. The open-state model of Kv1.2, which is 100% homologous with Kv1.5 in the inner vestibule (Fig. 1) and selectivity filter was used as the receptor [16]. The starting conformation of the ligand, vernakalant, was an energy minimized form. The channel was held rigid during the docking process while the ligand was allowed to be flexible. The grid box size was 18.75 Å × 18.75 Å × 37.5 Å in the *x*, *y* and *z* dimensions, with the centre of the grid corresponding to the central axis of the pore at threonine 480 at the base of the selectivity filter. Test runs expanding the grid beyond this size did not change which residues were predicted to interact with the drug.

Additional blind docking was carried out using AutoDock Vina [17] using a rigid receptor for comparison with AutoDock4 and also with flexible side chains for T479, T480, V505, I508 and V512. The grid size was the same as for the AutoDock4 docking and exhaustiveness was set at 50.

Mutations were made to the channel using the Swiss-PDBViewer V3.9b2 (DeepView; http://spdbv.vital-it.ch/) and then several residues surrounding the mutation were selected for energy minimization with DeepView also using the GROMOS96 implementation of Swiss-PdbViewer.

3. Results

3.1. The landscape of the inner vestibule with interacting residues

Our original study of mutations that affected the binding of vernakalant to Kv1.5, used the structure of Kv1.2, which is 100% homologous to Kv1.5 in the inner vestibule where the drug binds (Fig. 1), and predicted that residues T479, T480, V505 and I508 were potentially accessible for direct interaction with the drug [4]. The inner vestibule, highlighting the potential interacting surfaces for vernakalant, is shown in Fig. 1. In this diagram of two subunits of the channel, the front subunit and one side subunit have been removed to provide a clearer view of the inner vestibule. Identical residues from the subunits are colored similarly and the view extends from the selectivity filter at the top to the bundle crossing intracellularly. It can be seen that a widening of the inner vestibule is apparent underneath the internal entrance to the selectivity filter defined by T479 and T480. A pocket extends backwards and superiorly with M478 at its apex. It is these residues, between and including M478 to V512 in the four coordinated subunits that are predicted to variously form the binding site(s) for vernakalant in the simulations.

3.2. Using Autodock4 in long evaluation (LE) mode results in clustered binding conformations

In the present study, AutoDock4 was again used to further explore potential binding modes of vernakalant to the open-state Kv1.2 channel structure [16]. This included increasing the number and time allowed for each docking simulation and making point mutations in the channel using SwissPDB Viewer and re-running the docking simulations. Each AutoDock run not only predicted a binding conformation but also produced a value for free energy of binding (FEB) in kcal/mol and an estimated inhibitory concentration (K_i) in μM. It should be noted that these values do not take into consideration the intracellular solution that bathes the protein, the potential competition with potassium ions near the base of the filter, or the electric field in which the protein exists and which the drug is subjected to.

One of the user set variables in AutoDock is the time allowed for the program to look for an optimal binding site, and this is set by the maximum number of evals and maximum number of generations settings. Of course, the more evaluations allowed, the longer each simulation takes to run, and so the default setting is medium (2,500,000 evals, ME). This was increased to 25,000,000 evaluations (long evals, LE), as with an increasing number of torsional degrees of freedom in the ligand [18], this improves the chances of finding the lowest energy binding conformation. From the averaged free energy of binding and K_i values for 20 runs with the WT channel, giving Autodock more time to search for a binding site resulted in an average K_i that was 20 μM less than with the ME setting. Often the same residues were involved in the interactions with the drug, though in the ME run more interactions are seen distal to the pore at position V512 (data not shown).

A histogram is shown in Fig. 2 of 110 docking attempts, using the LE setting, that have been clustered into 34 bins based on positional similarity between atoms of an initial lowest free energy conformation and all the other conformations. Only conformations with a root-mean-square-displacement (RMSD) less than or equal to 3.0 Å from the initial root conformation are clustered together. For most docking studies it is expected that if AutoDock is given enough time to search, each run should converge on the same lowest energy binding site and thus all the results would cluster

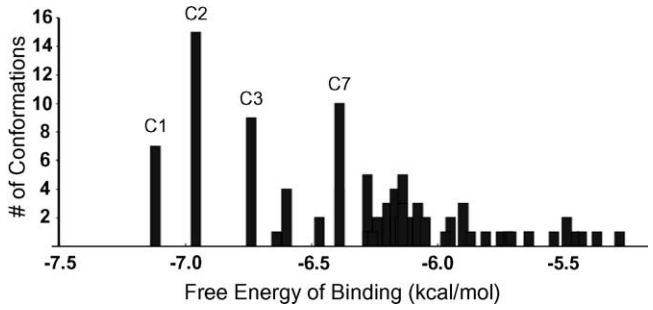

Fig. 2. Histogram of clustered vernakalant binding conformations using a RMSD of 3.0. Clusters are determined by root-mean-square-displacement between atoms in the lowest free energy conformations (which determines where the bar in the histogram is placed) and all other conformations. Those that are within 3.0 RMSD of the root conformation are included in the cluster despite having less favorable free energies of binding.

together. This is not necessarily what we would expect for vernakalant docking to Kv1.5, as Autodock is unable to take into account the fourfold symmetry, a result of identical subunits making up the channel, and therefore it is expected that several of the clusters in Fig. 2 actually represent the same binding conformation, i.e. the same residues and combinations, but involving different subunits. In addition, mean differences of FEB within about 2.5 kcal/mol are considered within the standard deviation of the free energy force field used by AutoDock4 to evaluate the energetics of binding conformations [15]. A summary showing the FEB, K_i, interacting residues and hydrogen bonds is shown for the 50 lowest energy conformations ranked in order from lowest to highest K_i in supplemental Figure S1.

If the conformations in each of the major low energy clusters are superimposed upon each other (Fig. 3) and viewed from the side (left) or above (middle), it is easy to see that they might represent similar conformations interacting with a different combination of subunits. For help in visualizing these conformations within the inner vestibule, the clusters are shown situated within the channel inner vestibule structure at the right, for conformations 1, 2, 3, and 7, from top to bottom in Fig. 3. After the root conformation 2-1 from cluster 2 is rotated 270° in the *y* plane and overlain on the root conformation from cluster 1 (1-1), MacPyMOL calculates a RMSD of 1.84 Å between these two conformations if two atoms are rejected and 1.74 Å if 5 atoms are rejected (Fig. 3C). If the root conformation from cluster 3-1 is rotated 180° in the *y* plane and superimposed upon the root conformation from 7-1 (Fig. 3F) the RMSD of the two conformations is 1.56 Å after MacPyMOL has rejected 2 atoms, and as low as 1.73 Å after rejection of only 1 atom. These results suggest that these four clusters of computed conformations can actually be collapsed into two larger clusters when the fourfold symmetry of the channel is taken into account. It is expected that further analysis of some of the other minor clusters would result in a similar amalgamation of conformations. If clusters 1 and 2 are grouped there are now 22 conformations and if clusters 3 and 7 are similarly grouped there are 19 after amalgamation. Both of these larger clusters represent highly possible binding sites for vernakalant, but beyond this analysis, preference can only be established by comparing the FEB.

3.3. Visualizing the channel-vernakalant conformation with the lowest FEB

The conformation with the most favorable FEB or lowest K_i is conformation 40, which is the root conformation of cluster 1 (Figs. 2–4). The FEB is −7.12 kcal/mol and the predicted inhibitory constant (K_i) is 6.08 μM. The view from various angles shows vernakalant's orientation within the inner vestibule and in this conformation the drug makes contact with all four T480 residues (Fig. 4). When examined from the side view (Fig. 4D and E) the drug appears to be clearly positioned to block the channel as it directly occludes the pore. Vernakalant appears to be folded upon itself with its ether linkage facing the T480 of three subunits (green, yellow and magenta) at the base of the selectivity filter. In this low energy conformation, vernakalant is predicted to make three hydrogen bonds with the channel (Fig. 4E and 5). The first bond is between the hydroxyl hydrogen of the pyrrolidinol (H-27 inset of Figure S1) and the carbonyl oxygen on M478 in subunit 3. The second H-bond is between the polar hydrogen on the nitrogen of the pyrolidine ring (H-21 inset of Figure S1) and the hydroxyl oxygen of the side chain of T480 in subunit 3. The third bond predicted is between the ether linkage oxygen of the ethoxy-cyclo hexyl group (O-7 in inset of Figure S1) and the hydroxyl hydrogen of the side chain of T480 in subunit 2. In other conformations, H-bonds with the channel were seen made from the methoxy oxygens and also the hydroxyl oxygen of the pyrrolidinol (Figure S1).

The frequency of interaction with various residues among the different conformations is shown in Fig. 6. The drug interacts most frequently with T480 with an average 87% occupancy amongst all conformations and 93% occupancy if only clusters 1, 2, 3 and 7 are considered. The percentage of interaction drops off to about 66 and 71% for V505, 45 and 49% for I508, 32 and 43% for T479, 5 and 9% for M478 for all conformations and the four clusters, respectively.

3.4. Flexible docking with AutoDock Vina

In addition to using AutoDock4 we also carried out blind docking with AutoDock Vina, a newer program developed by the makers of AutoDock [17]. This program was able to handle the docking of vernakalant (8 flexible bonds) with the channel in which the side chains of T479, T480, V505, I508 and V512 were allowed to be flexible (32 flexible bonds). The FEB for the flexible docking ranged from −17.8 to −13.0 kcal/mol for 30 conformations derived from 5 separate runs of the program. Using a rigid channel structure with Vina, resulted in values ranging from −7.3 to −7.0 kcal/mol for FEB, similar to the −7.12 kcal/mol predicted by AutoDock4 for conformation 40. The docking results from Vina predicted the same residues as AutoDock4 would interact with vernakalant except for M478. In general, there were fewer interactions high up against the pore and fewer hydrogen bonds predicted by Vina, both in the rigid channel molecular docking and in the flexible docking. 30% of rigid and 33% of flexible conformations had hydrogen bonds predicted as compared to 79% by AutoDock4. This is likely a contributing factor to the ∼44% reduction in interaction at T480, 24% at T479 and no interaction at M478 found with the flexible but not the rigid docking with Vina. The rate of interaction at T480 was the same for AutoDock4 and Vina rigid docking though Vina predicted a lower interaction rate with I508, this was entirely compensated for by a higher rate of interaction with V505. Vina also predicted a slightly higher interaction rate at V512.

In the conformation with the lowest FEB (conformation 5-1; −17.8 kcal/mol, Fig. 7) from the flexible docking, vernakalant makes contact with T480 in subunits 1–3, all four V505 residues and I508 from subunits 1 and 3 and thus sits high up in the inner vestibule like conformation 40 (Fig. 7A–C). When aligned in MacPyMOL the RMSD for conformation 40 and 5-1 is 1.57 Å (Fig. 7D and E), indicating a high degree of similarity between the most favored conformations from each of the programs. The RMSD for the conformation most favored by Vina from the rigid docking (conformation 1_1) vs. conformation 40 from AutoDock4 was 1.85 Å with 1 atom rejected and 0.95 Å with 4 atoms rejected.

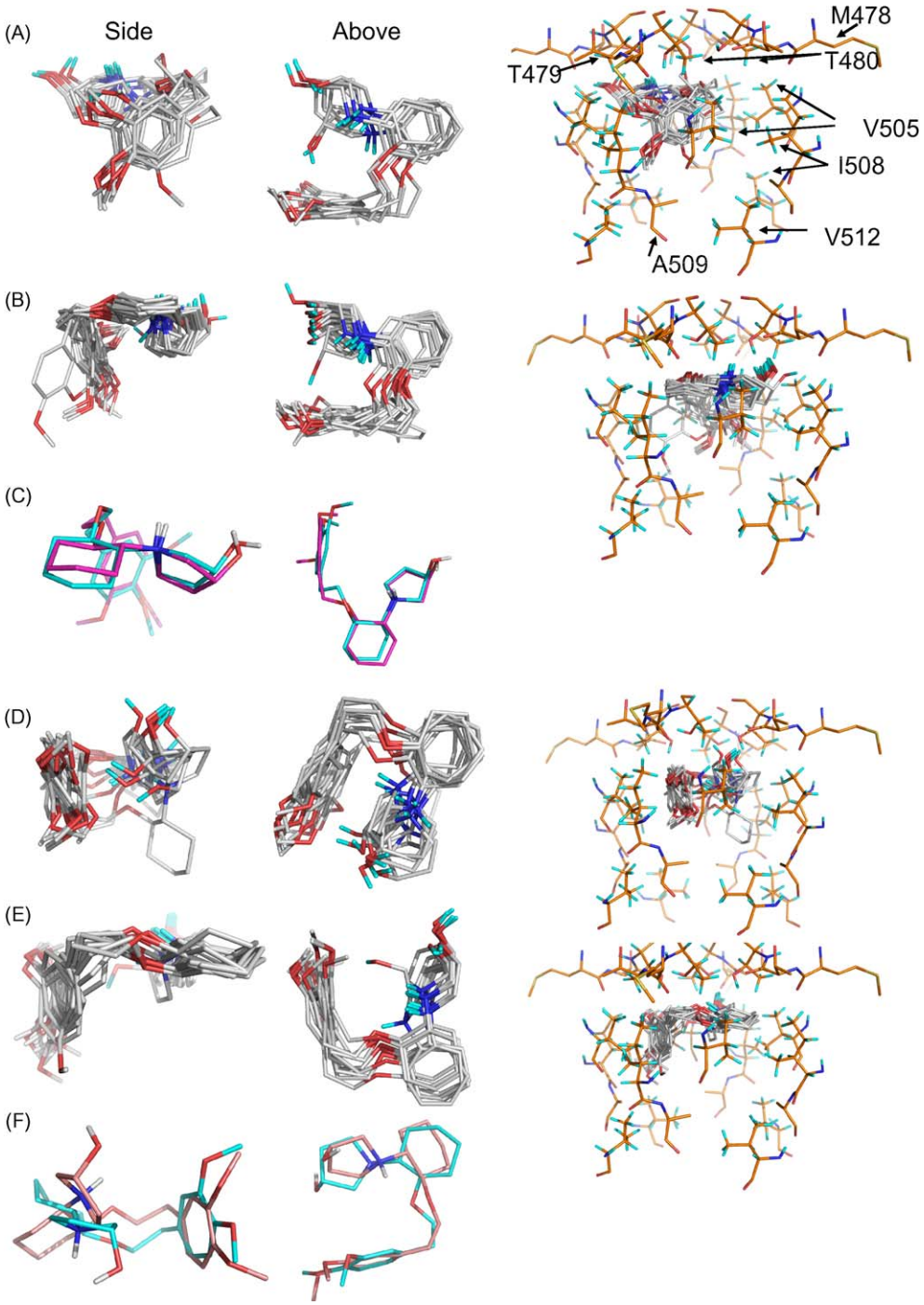

Fig. 3. Superimposed conformations of vernakalant from the four largest low energy clusters. Side and view from above (filter side) of superimposed conformations of vernakalant from cluster 1 (A), cluster 2 (B) cluster 3 (D) and cluster 7 (E), as well as each cluster docked into the channel structure. Only commonly interacting residues are shown (M478, T479, T480, V505, I508, A509 and V512) in stick format, as labeled in A. (C) Superimposition of conformation 1-1 and 2-1 with a 270° rotation or (F) 7-1 with a 180° rotation of 3-1 in the *y* plane shown from the side and from above.

3.5. Simulations of mutations affecting vernakalant binding

Our prior experimental studies provided the basis for understanding the molecular basis for block by vernakalant involving, as it did, most of the residues that the above modeling studies have suggested to be important in vernakalant binding [4]. Making these mutations in the crystal structure and re-docking vernakalant provided a unique test of the ability and scope of the model to accurately represent the experimental data. The model results of vernakalant docking to mutant channels allows prediction of inhibitory constants that can be compared with experimentally obtained IC_{50} values, and gives insight into likely changes in the interacting residues. To carry out these simulations, we made point mutations as in our earlier experimental alanine scan of the channel in the Swiss PDB Viewer, selected residues around the mutation and allowed the program to energy minimize. The differences in channel structure appear to be quite subtle as shown for mutation I508A (see Figure S2). This might be a result of the mutation being largely a reduction in side chain size which does not significantly alter the dominant constraints on the backbone structure.

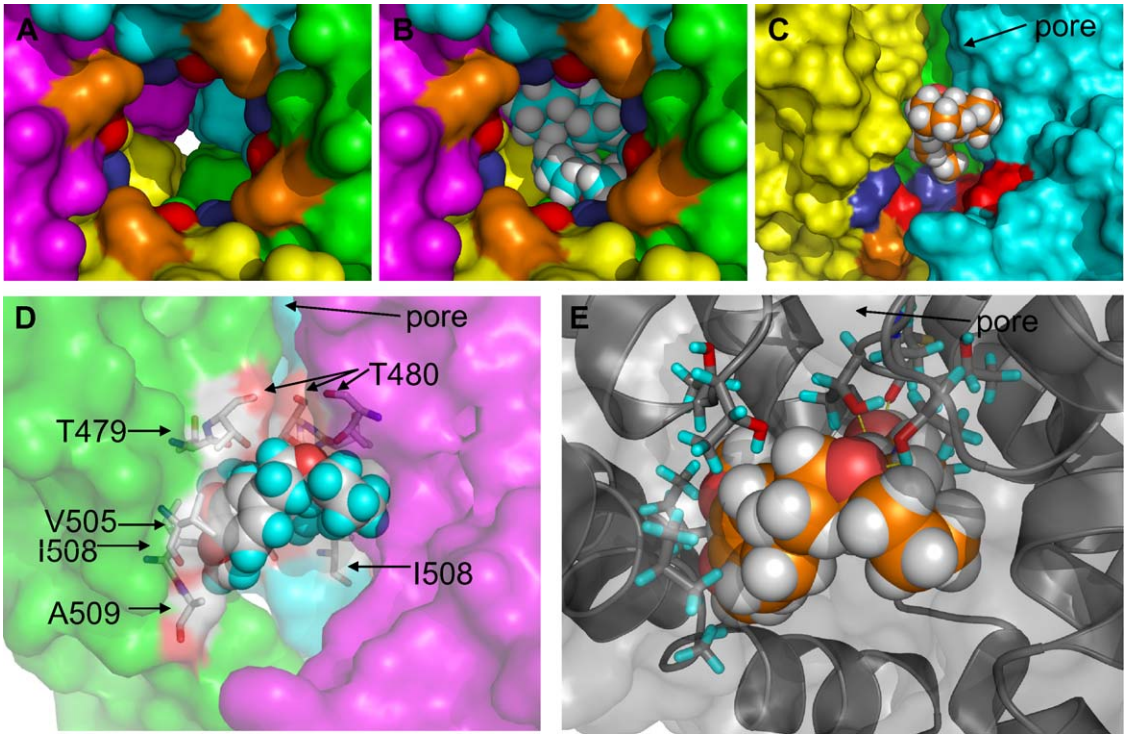

Fig. 4. Space-fill models of the lowest free energy conformation of vernakalant docked to molecular surface-represented channel. (A) Model of the inner vestibule (I502-V516) and deep pore (M478-T480) empty (A) and with drug docked (B) looking up towards the selectivity filter and from the side (C) where the front subunit has been removed for clarity. The channel is shown represented with a semitransparent molecular surface. In the lower panels, side chains of interacting residues are shown as sticks and the docked complex is viewed from the side (D) and again from the side but with *h*-bonds shown (yellow dashed lines) and the channel in also cartoon format (E). It can be seen that the ethoxy group (red oxygen atom) figures prominently as an obstruction in the ion pathway. In (A)–(C), V512 is colored red, A509 in deep blue and P513 in orange to delineate the lower regions on the inner vestibule.

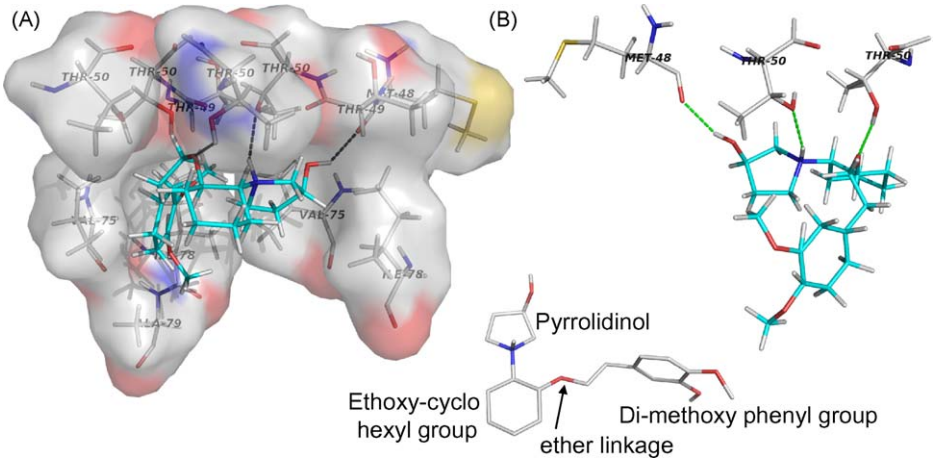

Fig. 5. In the lowest energy AutoDock conformation (40), vernakalant is predicted to make three hydrogen bonds with the channel. (A) Model of docked vernakalant showing all interacting channel residues from conformation 40, shown here in stick and semitransparent surface representation. Hydrogen bonds are shown by black dotted lines. Interacting residues include T480 from subunit 1 and 2, M478, T479, T480, V505 and I508 from subunit 3 and T479, T480, V505, I508 and A509 from subunit 4. (B) Only channel residues involved in predicted hydrogen bonds are shown here in stick representation with the hydrogen bonds represented as green dotted lines and the carbons of vernakalant shown in cyan. Inset is a stick representation of vernakalant with only polar hydrogens shown.

The box-and-whisker plot in Fig. 8 presents comparisons of mutant vs. WT K_i's for vernakalant, though it should be noted that the mutants have been subjected to lower numbers of AutoDock runs than WT, simply for economy of computing time. For WT, T480A, V505A and I508A the IC_{50} values for block all sit somewhere on the range of predicted K_i's, generally below the median value. Values were very similar to those found for the Kv1.2 (WT) structure when the pore domain of the Kv1.2–2.1 paddle chimera model [19] was used for the docking simulations, though they grouped more tightly. The numbers show a somewhat similar trend of increasing K_i values as was seen with the IC_{50}s for block, with the mutations to those residues in the middle range of the binding site (V505 and I508) showing the greatest dispersion. Vernakalant appears able to bind similar combinations of residues when the T480A mutation is made, including the same rate of interaction with the residue at 480 (Fig. 9). The increase in K_i likely comes from the loss of the normally high rate of hydrogen bonding with the hydroxyl group at this position. The WT, V505A and I508A

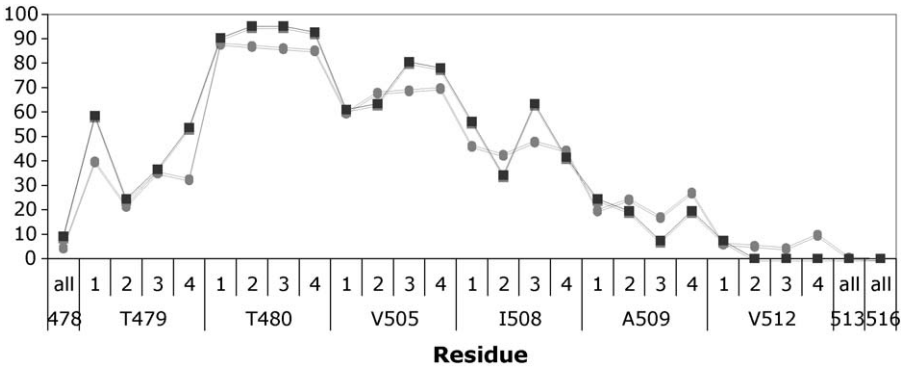

Fig. 6. Summary of vernakalant contacts with given residues as a percentage of conformations. The grey circles represent all 110 conformations and the black squares include only clusters 1, 2, 3, and 7 from Fig. 2. Numbers above each amino acid residue indicates the subunit involved.

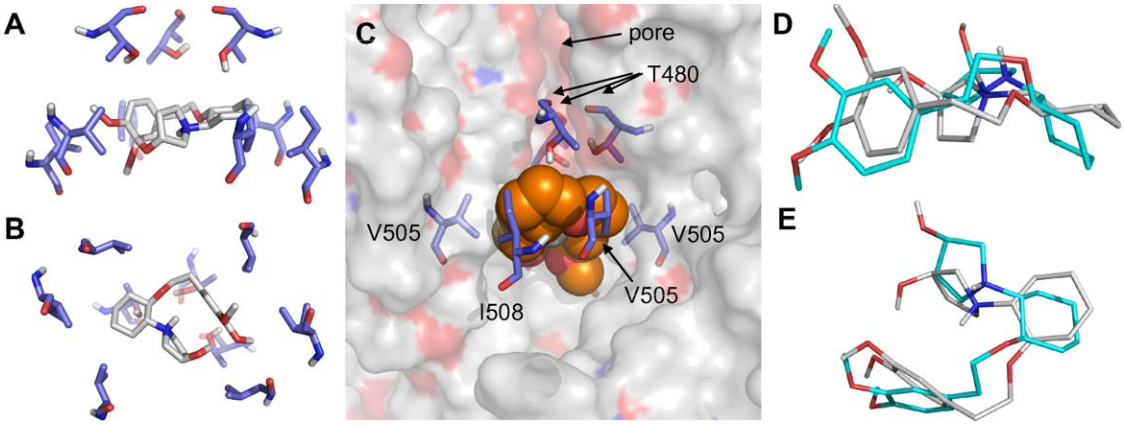

Fig. 7. Lowest free energy of binding conformation, conformation 5-1, from flexible docking with AutoDock Vina. Conformation 5-1 along with interacting residues in stick format shown from the side (A) and from below (B) looking up towards the selectivity filter. (C) Conformation 5-1 again with the channel represented with a semitransparent molecular surface and interacting residues shown as sticks, viewed from the side and the front subunit removed for clarity. (D) Alignment of conformation 40 (carbons in cyan) from the AutoDock4 docking with conformations 5-1 (carbons in grey) shown from the side and from above (E).

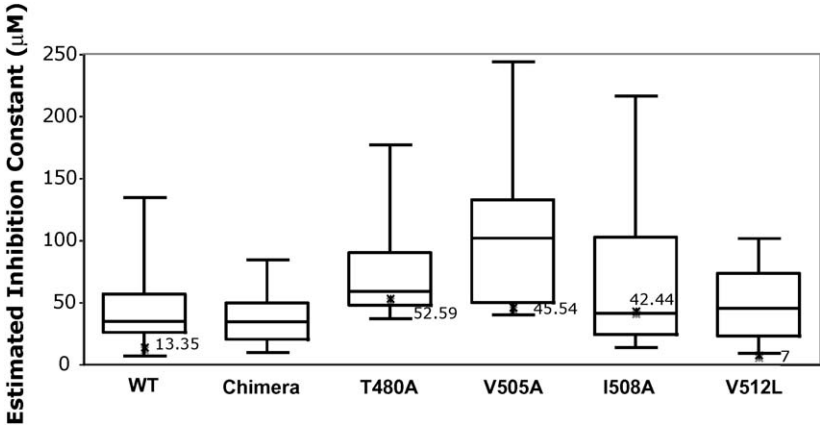

Fig. 8. Box-and-whisker plot of K_i values for all AutoDock predicted vernakalant binding conformations to WT and mutant Kv1.5 channels. The boxed region denotes the 25th to 75th percentiles and is bisected by the median value. The extremities represent the minimum and maximum values. The ✖ represents the IC50 values from patch-clamp experiments ([4], Table 1). Number of runs for each are: WT = 110; Chimera = 50; T480A, V505A, I508A and V512L = 30. Median values in μM for the different constructs: WT, 33.9; Chimera, 33.50; T480A, 57.9; V505A, 101; I508A, 40.5; V512A, 44.44.

have rates of 80, 83 and 73% of conformations with at least one hydrogen bond with the drug, the T480A mutant has only a 40% rate (data not shown). The increase in K_i for V505 (Fig. 8), appears related to the loss of interaction at V505, where it goes from a rate of 65% in WT to about 45% in V505A without any real additional compensation at other residues (Fig. 9). The I508A mutation results in only a 10% decrease in interaction at position 508 but there is a 20% increase in interaction at M478 and 30% of these interactions are as part of a hydrogen bond with the backbone carbonyl of M478. Of the 8 conformations not making hydrogen bonds with the I508A mutant channel, 6 of these are found beyond the 75th percentile for K_i. The occupancy at T480 was slightly lower, at 83%,

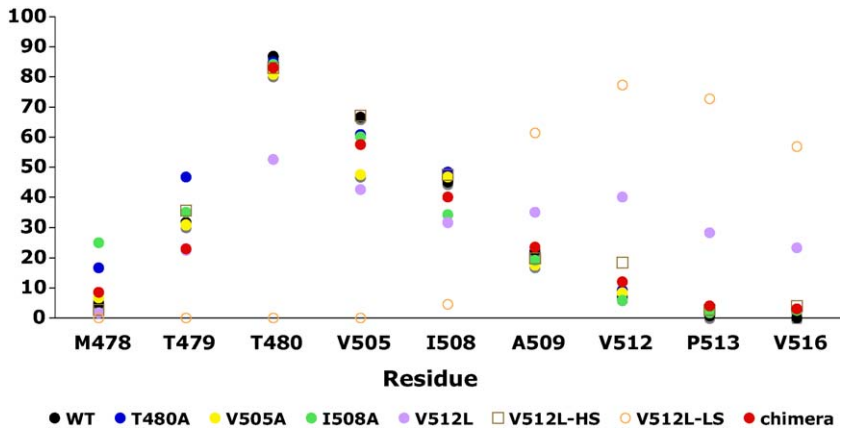

Fig. 9. Frequency of interaction of vernakalant with given residues in wild-type and mutant channels. All 4 subunit totals were summed together. Number of runs for each are: WT = 110; Chimera = 50; T480A, V505A, I508A and V512L = 30. V512L is further divided into a high binding site (V512L-HS) and a lower binding site (V512L-LS) which includes 19 and 11 conformations, respectively.

when the pore domain of the chimera model was used for the docking simulations, and may be explained by the observation that vernakalant made slightly more interactions lower down the inner vestibule at V512 and P513 (Fig. 9).

We found that putting a slightly bulkier, more hydrophobic leucine at 512 made Kv1.5 slightly more sensitive to vernakalant, having and IC_{50} of ~7 μM, though this did not reach significance [4]. When this same mutation was tested using AutoDock, the lowest K_i, 8.04 μM, was remarkably close to this predicted IC_{50} (Fig. 8). Not only did vernakalant make contact more frequently overall with L512 (40% compared to 10% for WT; Fig. 9) but it also makes contact in this lowest FEB conformation. The other interesting feature of putting a bulkier residue at 512 is that it creates two distinct binding patterns, those that encompass T480 and the upper vestibule (Fig. 9, V512L-HS) and those that do not (Fig. 9, V512L-LS). The average FEB for all the conformations involving T480 was −6.23 kcal/mol and for all those that did not bind above A509, the average K_i was −5.67 kcal/mol. No other mutation resulted in such a clear separation of binding domains, nor was this ever observed in the WT channel (Fig. 10).

For the WT channel, only 3 out of the 11 lowest energy conformations (out of a total of 110) make contact with M478. Two mutations were also attempted at M478, but unfortunately neither an alanine nor a glycine at this position resulted in functional expression of the channel.

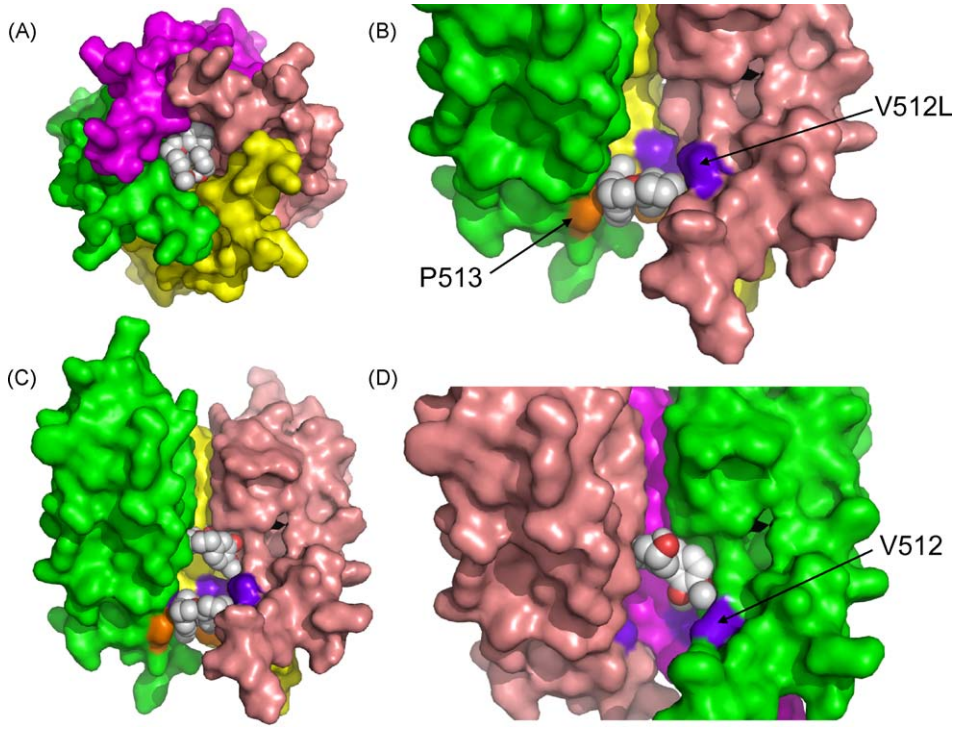

Fig. 10. Interactions at residue 512. (A) Surface model of the channel with V512L mutation, looking up from the cytoplasmic side showing vernakalant docked in the lower binding site. (B) Same as in (A) but viewed from the side, with the front subunit removed. Leucine 512 is colored purple-blue and the proline at 513 is colored orange. (C) Shows a vernakalant molecule docked in the higher site as well as the low site, illustrating the separation between the two sites. (D) Shows conformation 68, belonging to cluster 2 (Fig. 3) docked into the WT channel, interacting at V512 (colored purple-blue) in the green subunit.

4. Discussion

4.1. Use of the Kv1.2 model

The homology models used in recent years to examine the binding of ligands within the inner vestibule of Kv1.5 channels have generally used the KcsA structure for pharmacophore design [20,21], which is not ideal for Kv1 channels as there is only 36% sequence identity between KcsA and Kv1.5, and this structure is thought to represent the closed state. Others have used a combination of KcsA and MthK [21,22], or a KcsA-based Kv1.3 pore homology model for the binding of specific Kv channel blockers, S0100176 and AVE0118 [10,11]. More recently the Kv1.2 crystal structure has been used as a homology model of Kv1.5, to develop new Kv1.5 blocking agents for the treatment of atrial fibrillation [23], and also for studies of ligand docking into the channel [24,25]. Residues, T479 and T480 at the base of the selectivity filter, as well as residues extended down S6, V505, I508, for S0100176, and V512, for Kv1.5 antagonists S9947 and ICAGEN-4 [24] and even beyond to V516 for the more extended conformations of AVE0118, have been identified, by both alanine mutational analysis and modeling, as important for drug binding. Although the T480A mutation was found to affect binding in experimental studies with S9947 and ICAGEN-4, the docking model suggested drug coordination with the innermost potassium ion in the selectivity filter, as observed for block of Kv1.3 by correolide and chromanol-293 block of KCNQ1 [26,27].

In the present study we primarily used the Kv1.2 model [16], since Kv1.5 has an identical sequence in the drug-accessible intracellular vestibule and selectivity filter region (Fig. 1). In Fig. 1, the architecture and the available interaction surface of this region immediately show why all experimental studies and many of the modeling studies have identified similar residues as important sites for drug binding.

Different modeling systems have then been used to dock ligands in the homology models. For S0100176, the ligand was manually docked to the putative site in the central cavity, a short sequence of energy minimizations was carried out to remove severe steric clashes with the protein, and potential contacts were defined as those less than 4.5 Å between the ligand and any of the side chain atoms [10]. Docking of AVE0118 was carried out using a similar methodology and the KcsA-based Kv1.3 homology model, but using GOLD [11]. Others have used a combination of manual docking criteria [28] usually with some kind of energy optimization, for example the Global Range Molecular Matching program [24], or an 'active site' chosen around I508 and V512 into which docking was performed using DOCK 5.4 [23], or with an active site radius of 22 Å centered around a point on the symmetry axis of the channel slightly above the PVP region of S6 [25].

Here, we used an Autodock4 docking grid that encompassed the majority of the S6 domains of the channel without further bias, which included the entire intracellular vestibule of the channel and selectivity filter, and the extracellular S6 beyond the intracellular activation gate, defined by the PVP sequence at 512.

4.2. Description of four clustered binding conformations and their rotational similarities

From 110 docking runs, four major binding conformations were identified, clustering together those with less than 3.0 Å RMSD between atoms from each other (Fig. 2). Of these conformations, 1 and 2 and 3 and 7 were found to be simple rotamers of each other, occurring as a result of the homotetrameric structure of the channel. Thus, 41 of the 110 conformations including the lowest energy conformation, fell into two roughly equal-sized structural groups, as shown in Fig. 3. In all of these conformations, oxygen in the ether linker of vernakalant or in the methoxy groups, form hydrogen bonds with hydroxyl hydrogens in the channel residue side chains, of especially T480, or alternatively, the hydroxyl hydrogens in vernakalant form hydrogen bonds with backbone carbonyl oxygens of M478, T479, T480 or V505 as shown in the bond table in Figure S1. The stability of these kind of bonds lead to the prediction that the drug is going to bind high up in the inner cavity up against the inside of the selectivity filter, as shown in the depiction of a large number of the conformations of vernakalant in the ball and stick models in Fig. 3.

The table in Figure S1 indicates that in all of the lowest (most favored) FEB conformations of vernakalant, the drug binds the T480 residue in all four subunits, and this is the most completely bound residue in all the conformations analyzed. Even in conformations with higher FEB's, this residue is often bound in all four subunits. Thus, in the summary graph of vernakalant contacts with different residues (Fig. 8) it can be seen that T480 is bound between 85 and 95% of the time. The only other residue for which this is the case is V505, which is bound in all four subunits in 10 of the top 50 conformations (Figure S1), and between 60 and 80% of the time otherwise (Fig. 8). Other residues are bound less often, with I508 bound less than 50% of the time and A509 less than 20% of the time, with V512 rarely bound in any of the four subunits. Again these data support the idea that vernakalant binds high up in the inner vestibule of the channel in almost all conformations. Blind flexible docking with AutoDock Vina did result in predictions of much less interaction at T480, T479 and none at M478 in the 30 conformations examined but the lowest FEB conformation, 5-1 showed a similar binding site higher up in the inner vestibule (Fig. 7). This is similar to the location within the channel described for S0100176 [10], but different from almost all other experimental and modeling studies of drug binding to Kv1.5 channels in which an extended conformation along S6 is predicted for drugs as diverse as AVE0118, disubstituted bisaryl compounds, S9947, MSD-D, and ICAGEN-4 [11,20,24,25]. We cannot rule out that vernakalant may start in a more extended conformation and make contact with V512, perhaps even temporarily. It is clearly possible for the drug to make contact with all four T480 residues and with V512 in one subunit in a low energy conformation, such as number 68 (Figure S1 and Fig. 10D), which has a FEB of −6.90 kcal/mol and is within the same cluster as number 40 after rotation (Fig. 3). When a truncated version of the chimera model was used, V512 was bound slightly more frequently with a 12% occupancy rate, but only in less favored conformations above the median FEB value (data not shown). Interestingly, when the two structures are compared, it appears as though the Kv1.2 structure is slightly narrower than the chimera in the inner vestibule (Figure S3).

4.3. Depiction of the conformation with the lowest free energy of binding

Conformation 40 and conformation 5-1 from the flexible docking, (Fig. 7E) shows that, rather than being in an extended conformation, vernakalant appears to show flexibility about the ethoxy linker and this has the effect that the drug is folded upon itself allowing the ether oxygen to bond with side chains of T480. This forms a compact configuration when viewed from below or the side (Figs. 4 and 7) that closely approximates to the internal side of the selectivity filter. In addition to hydrophobic and van der Waals interactions (Fig. 5, Figure S1), three hydrogen bonds are formed between vernakalant and the channel (Fig. 5), those with T480 mentioned before, and one with M478. This last finding was something of a surprise as M478 has only a minor presence in the inner cavity as shown in Fig. 1, and in our previous mutational work we had not attempted mutations here [4]. Mutations at this site made subsequently to test for a role in binding did not express,

making it impossible to assess the true role of M478. Conformation 40, depicted in Figs. 4 and 5 is not unique, as Autodock4 predicted interactions with M478 in other conformations also (Figure S1). This result was not reproduced by AutoDock Vina, however, a program with a different search algorithm and scoring function than AutoDock4 [17].

4.4. Simulating experimental mutational results using Autodock4

Incorporation of mutations into the Kv1.2 channel model allowed us to make a comparison between the electrophysiological effects of mutations made experimentally and in simulations with Autodock4. These are tentative as the electrophysiological IC_{50} is a measure of the ability of the drug to pass across the membrane and block the channel, whereas the K_i obtained from Autodock4 simulations is the estimated inhibitory constant of the drug at a particular site if it is the only one bound. Those wild-type residues found to bind vernakalant in blind docking simulations include all those that, when mutated, were found to affect the potency of vernakalant—with the exception of I502 [4]. Specifically, alanine substitutions of T480, V505, and I508, but not V512L, all reduced vernakalant potency in the rank order of IC_{50}: V512L < WT < I508A < V505A < T480A (Fig. 8, and [4]), and interacted with the drug in Autodock4 simulations (Figs. 3 and 4). It should be noted that A509 is also suggested to form part of the vernakalant binding site, in some conformations (Figure S1), whereas no effect of A509G mutation was found in experimental studies. This is not surprising given that this substitution represents a retraction in side chain mass which likely then would not force a repositioning of the drug with respect to other residues. Overall, the conservative alanine mutations within the cavity had quite small effects on the frequency of predicted binding to different residues (Fig. 9) and on vernakalant potency, increasing IC_{50} values 3–4-fold, but still Autodock4 simulations reproduced the rank order of change in potency very closely, with the exception that the position of V505A and T480A were reversed.

In our earlier mutational studies we had found that mutation of I502 to Ala greatly reduced the potency of vernakalant binding to the channel, from 13 to 330 μM, and to 150 μM for I502F [4]. I502 is not apparent in the binding cavity (Fig. 1), and docking studies did not predict interactions with I502 (Figure S1). Thus, we conclude that mutations at this site alter channel architecture sufficiently to disrupt drug binding, rather than I502 itself being an integral part of the binding domain

Simulation of V512L reproduced the slightly increased potency seen experimentally (56% block at 10 μM, compared with 45% for WT channels [4]). This mutation created a distinct lower binding site (Figs. 9 and 10A–C) not seen with any other mutation or in the WT channel, which tended to show more of a continuum of binding conformations. Perhaps by putting this bulkier residue here it creates steric hindrance for movement into the deeper vestibule. Movement from this lower site during the AutoDock run may then depend on whether vernakalant is in a more extended form or folded upon itself. The lowest K_i for this lower binding site in the V512L mutant channel was 40.04 μM.

5. Conclusion

Use of the blind docking tool AutoDock4 has proven remarkably useful in understanding the spatial and drug binding landscape of the channel, as well as providing plausible binding conformations for vernakalant. While there are factors that the program cannot account for at this time, such as the electric field, potassium occupancy and the flexibility of the channel during drug–channel interactions and during the gating process, it has matched experimental mutational studies in its predictions for important interacting residues for vernakalant.

Acknowledgements

We thank Dr. Grace Jung for help with the energy minimized form of vernakalant. This work was supported by a research grant from Cardiome Pharma Corp, and operating grants from the CIHR and the Heart and Stroke Foundations of British Columbia and Yukon. DF was supported by a Career Investigator Award from the Heart and Stroke Foundation of Canada.

Appendix A. Supplementary data

Supplementary data associated with this article can be found, in the online version, at doi:10.1016/j.jmgm.2009.07.005.

References

[1] D. Roy, B.H. Rowe, I.G. Stiell, B. Coutu, J.H. Ip, D. Phaneuf, J. Lee, H. Vidaillet, G. Dickinson, S. Grant, A.M. Ezrin, G.N. Beatch, A randomized, controlled trial of RSD1235, a novel anti-arrhythmic agent, in the treatment of recent onset atrial fibrillation, J. Am. Coll. Cardiol. 44 (2004) 2355–2361.
[2] D. Roy, C.M. Pratt, C. Torp-Pedersen, D.G. Wyse, E. Toft, S. Juul-Moller, T. Nielsen, S.L. Rasmussen, I.G. Stiell, B. Coutu, J.H. Ip, E.L. Pritchett, A.J. Camm, Vernakalant hydrochloride for rapid conversion of atrial fibrillation: a phase 3, randomized, placebo-controlled trial, Circulation 117 (2008) 1518–1525.
[3] I. Savelieva, J. Camm, Anti-arrhythmic drug therapy for atrial fibrillation: current anti-arrhythmic drugs, investigational agents, and innovative approaches, Europace 10 (2008) 647–665.
[4] J. Eldstrom, Z. Wang, H. Xu, M. Pourrier, A. Ezrin, K. Gibson, D. Fedida, The molecular basis of high-affinity binding of the antiarrhythmic compound vernakalant (RSD1235) to Kv1.5 channels, Mol. Pharmacol. 72 (2007) 1522–1534.
[5] D. Fedida, P.M.R. Orth, J.Y.C. Chen, S. Lin, B. Plouvier, G. Jung, A. Ezrin, G.N. Beatch, The mechanism of atrial antiarrhythmic action of RSD1235, J. Cardiovasc. Electrophysiol. 16 (2005) 1227–1238.
[6] D. Fedida, Vernakalant (RSD1235): a novel, atrial-selective antifibrillatory agent, Expert Opin. Investig. Drugs 16 (2007) 519–532.
[7] D. Fedida, B. Wible, Z. Wang, B. Fermini, F. Faust, S. Nattel, A.M. Brown, Identity of a novel delayed rectifier current from human heart with a cloned K^+ channel current, Circ. Res. 73 (1993) 210–216.
[8] J.L. Feng, B. Wible, G.R. Li, Z.G. Wang, S. Nattel, Antisense oligodeoxynucleotides directed against Kv1.5 mRNA specifically inhibit ultrarapid delayed rectifier K^+ current in cultured adult human atrial myocytes, Circ. Res. 80 (1997) 572–579.
[9] R. Caballero, I. Moreno, T. Gonzalez, C. Valenzuela, J. Tamargo, E. Delpon, Putative binding sites for benzocaine on a human cardiac cloned channel (Kv1.5), Cardiovasc. Res. 56 (2002) 104–117.
[10] N. Decher, B. Pirard, F. Bundis, S. Peukert, K.H. Baringhaus, A.E. Busch, K. Steinmeyer, M.C. Sanguinetti, Molecular basis for Kv1.5 channel block: conservation of drug binding sites among voltage-gated K^+ channels, J. Biol. Chem. 279 (2004) 394–400.
[11] N. Decher, P. Kumar, T. Gonzalez, B. Pirard, M.C. Sanguinetti, Binding site of a novel Kv1.5 blocker: a "foot in the door" against atrial fibrillation, Mol. Pharmacol. 70 (2006) 1204–1211.
[12] D. Herrera, A. Mamarbachi, M. Simoes, L. Parent, R. Sauve, Z. Wang, S. Nattel, A single residue in the S6 transmembrane domain governs the differential flecainide sensitivity of voltage-gated potassium channels, Mol. Pharmacol. 68 (2005) 305–316.
[13] S.W. Yeola, T.C. Rich, V.N. Uebele, M.M. Tamkun, D.J. Snyders, Molecular analysis of a binding site for quinidine in a human cardiac delayed rectifier K^+ channel—role of S6 in antiarrhythmic drug binding, Circ. Res. 78 (1996) 1105–1114.
[14] G.M. Morris, D.S. Goodsell, R.S. Halliday, R. Huey, W.E. Hart, R.K. Belew, A.J. Olson, Automated docking using a Lamarckian genetic algorithm and an empirical binding free energy function, J. Comput. Chem. 19 (1998) 1639–1662.
[15] R. Huey, G.M. Morris, A.J. Olson, D.S. Goodsell, A semiempirical free energy force field with charge-based desolvation, J. Comput. Chem. 28 (2007) 1145–1152.
[16] S.B. Long, E.B. Campbell, R. MacKinnon, Crystal structure of a mammalian voltage-dependent *Shaker* family K^+ channel, Science 309 (2005) 897–903.
[17] O. Trott, A.J. Olson, AuoDock Vina: improving the speed and accuracy of docking with a new scoring function, efficient optimization, and multithreading, J. Comput. Chem. (June) (2009) (Epub ahead of print).
[18] C. Hetenyi, S.D. van der, Efficient docking of peptides to proteins without prior knowledge of the binding site, Protein Sci. 11 (2002) 1729–1737.
[19] S.B. Long, X. Tao, E.B. Campbell, R. MacKinnon, Atomic structure of a voltage-dependent K^+ channel in a lipid membrane-like environment, Nature 450 (2007) 376–382.
[20] B. Pirard, J. Brendel, S. Peukert, The discovery of Kv1.5 blockers as a case study for the application of virtual screening approaches, J. Chem. Inf. Model. 45 (2005) 477–485.

[21] H.L. Liu, C.W. Chen, J.C. Lin, Homology models of the tetramerization domain of six eukaryotic voltage-gated potassium channels Kv1.1–Kv1.6, J. Biomol. Struct. Dyn. 22 (2005) 387–398.
[22] V.B. Luzhkov, J. Nilsson, P. Arhem, J. Aqvist, Computational modelling of the open-state Kv 1.5 ion channel block by bupivacaine, Biochim. Biophys. Acta 1652 (2003) 35–51.
[23] Q. Yang, L. Du, X. Wang, M. Li, Q. You, Modeling the binding modes of Kv1.5 potassium channel and blockers, J. Mol. Graph. Model. 27 (2008) 178–187.
[24] N. Strutz-Seebohm, I. Gutcher, N. Decher, K. Steinmeyer, F. Lang, G. Seebohm, Comparison of potent Kv1.5 potassium channel inhibitors reveals the molecular basis for blocking kinetics and binding mode, Cell. Physiol. Biochem. 20 (2007) 791–800.
[25] M. Ander, V.B. Luzhkov, J. Aqvist, Ligand binding to the voltage-gated Kv1.5 potassium channel in the open state—docking and computer simulations of a homology model, Biophys. J. 94 (2008) 820–831.
[26] I. Bruhova, B.S. Zhorov, Monte Carlo-energy minimization of correolide in the Kv1.3 channel: possible role of potassium ion in ligand–receptor interactions, BMC Struct. Biol. 7 (2007) 5.
[27] C. Lerche, I. Bruhova, H. Lerche, K. Steinmeyer, A.D. Wei, N. Strutz-Seebohm, F. Lang, A.E. Busch, B.S. Zhorov, G. Seebohm, Chromanol 293B binding in KCNQ1 (Kv7.1) channels involves electrostatic interactions with a potassium ion in the selectivity filter, Mol. Pharmacol. 71 (2007) 1503–1511.
[28] I.A. Vakser, C. Aflalo, Hydrophobic docking: a proposed enhancement to molecular recognition techniques, Proteins 20 (1994) 320–329.